

AINet+: Advancing Superpixel Segmentation via Cascaded Association Implantation

Yaxiong Wang, Yunchao Wei, Yujiao Wu, Xueming Qian *Member IEEE*, Li Zhu, and Yi Yang

Abstract—Superpixel segmentation has seen significant progress benefiting from the deep convolutional networks. The typical approach entails initial division of the image into grids, followed by a learning process that assigns each pixel to adjacent grid segments. However, reliance on convolutions with confined receptive fields results in an implicit, rather than explicit, understanding of pixel-grid interactions. This limitation often leads to a deficit of contextual information during the mapping of associations. To counteract this, we introduce the Association Implantation (AI) module, designed to allow networks to explicitly engage with pixel-grid relationships. This module embeds grid features directly into the vicinity of the central pixel and employs convolutional operations on an enlarged window, facilitating an adaptive transfer of knowledge. This approach enables the network to explicitly extract context at the pixel-grid level, which is more aligned with the objectives of superpixel segmentation than mere pixel-wise interactions. By integrating the AI module across various layers, we enable a progressive refinement of pixel-superpixel relationships from coarse to fine. To further enhance the assignment of boundary pixels, we’ve engineered a boundary-aware loss function. This function aids in the discrimination of boundary-adjacent pixels at the feature level, thereby empowering subsequent modules to precisely identify boundary pixels and enhance overall boundary accuracy. Our method has been rigorously tested on four benchmarks, including BSDS500, NYUv2, ACDC, and ISIC2017, and our model can achieve competitive performance with comparison methods.

Index Terms—Superpixel segmentation, Segmentation, Deep Learning, Stereo Matching.

I. INTRODUCTION

Superpixels are image regions formed by grouping image pixels similar in color and other low-level properties, which could be viewed as an over-segmentation of image. The process of extracting superpixels is known as superpixel segmentation. Comparing to pixels, superpixel provides a more effective representation for image data. With such a compact representation, the computational efficiency of vision algorithms could be improved [13], [19], [29], [32], [50], [59]. Consequently, superpixel could benefit many vision tasks like image recognition [13], [73], semantic segmentation [3], [20], [67], [75], [76], [79], object detection [15], [53], image denosing [47], optical flow estimation [23], [45], [57], [66],

Conference version of this work has been accepted by ICCV 2021.

Y. Wang is with the Hefei University of Technology, Hefei, 230000, China Email: wangyx@hfut.edu.cn.

Y. Wei is with the School of Information Science, Beijing Jiaotong University, Beijing, 100000, China. Email: wycho1987@gmail.com.

Y. Wu is with the CSRIO, Australia, Email: yujiaowu111@gmail.com.

X. Qian, and L. Zhu is with the Xi’an Jiaotong University, Xi’an, 710049, China. Email: {qianxm, zhuli}@mail.xjtu.edu.cn.

Y. Yang is with the School of Computer Science and Technology, Zhejiang University, Hangzhou, 310000, China, Email: yangyics@zju.edu.cn.

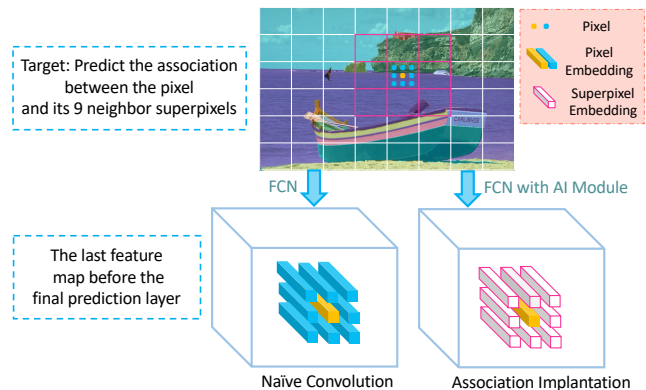


Fig. 1: Different from the SCN [68] that implicitly learns the association using the stacked naïve convolutions, we propose to implant the corresponding grid features to the surrounding of the pixel to explicitly perceive the relation between each pixel and its neighbor grids.

and even adversarial attack [12] and domain adaption [17] can benefit from superpixels. In light of the fundamental importance of superpixels in computer vision, superpixel segmentation attracts much attention since it is first introduced by Ren and Malik [51] in 2003.

The common practice for superpixel segmentation is to first split the image into grid cells and then estimate the membership of each pixel to its adjacent grids, by which the grouping could be performed. Meanwhile, the membership estimation plays the key role in superpixel segmentation. Traditional approaches usually utilize the hand-craft features and estimate the relevance of pixel to its neighbor grids based on clustering or graph-based methods [1], [2], [38], [42], [44]. For example, the classic method SLIC [1] treats the surrounding grids as the center candidates and perform clustering procedure on the image. While the ERS [42] models the superpixel as a random walk problem, which is also a popular strategy in traditional superpixel segmentation. However, these methods all suffer from the weakness of the hand-craft features and are difficult to integrate into other trainable deep frameworks. Inspired by the success of deep neural networks in many computer vision problems, researchers recently attempt to adopt the deep learning technique to superpixel segmentation [25], [34], [35], [68], [74], [77]. As mentioned in abstract, previous deep methods attempt to assign pixels by learning the association of each pixel to its surrounding grids using the fully convolutional networks [54]. The popular solutions like SCN [68], SSN [25] employ the U-net architecture [52] to predict the association, *i.e.*, the 9-way probabilities, for each pixel. Although stacking

convolution layers can enlarge the receptive field and help study the *pixel-grid wise* probabilities, introducing low-level features with skip connection in the final layer will pollute the probabilities due to the added *pixel-pixel wise* information, since the ultimate target is to predict the association between the target pixel and *its 9-neighbor grids* instead of its 9-neighbor pixels.

To tackle this weakness, we propose to directly implant the grid features to the surrounding of the corresponding pixel using an association implantation (AI) module. Fig. 1 simply shows the core idea of our AI module, before feeding the last features into the prediction layer, our AI module is performed: for each pixel, we place the corresponding grid features to its neighbors, then a convolution with 3×3 kernel is followed, this convolution is no longer to capture the pixel-pixel relation but *the relation between pixel and its 9 neighbor grids*, providing the consistent context with the target of superpixel segmentation. Our proposed AI module provides a simple and intuitive way to allow the network to harvest the pixel-neighbor grids context in an explicit fashion, which is exactly required by superpixel segmentation. Comparing to existing methods, such a design is more consistent with the target of superpixel segmentation and could give more beneficial support for the subsequent association map inferring. To further boost the performance, we employ our proposed AI module in the penultimate and the last layers, such that a hierarchical pixel-grid relation could be perceived, which could make the performance step further.

Besides, a satisfactory superpixel algorithm should accurately identify the boundary pixels, however, some designs towards this target still missed among existing works. To pursue better boundary precision, we augment the optimization with a boundary-perceiving loss. To be specific, we first sample a set of small local patches on the pixel embedding map along the boundaries. Then, the features with the same/different labels in each patch are treated as the positive/negative samples, on which a classification procedure is performed to enhance the compactness of the features with the same label while distinguish the different semantic features. Our boundary-perceiving loss encourages the model to pay more attention to discriminate the features around boundaries, consequently, more boundary pixels could be identified.

Quantitative and qualitative results on BSDS500 [4], NYUv2 [55], ISIC-2017 [9] and ACDC [28] datasets demonstrate that the proposed method achieves more outstanding performance against the state-of-the-art superpixel segmentation methods. In summary, we make the following contributions in this work:

- We propose a novel AI module to directly capture the relation between the pixel and its surrounding grid cells, such a design builds a more consistent architecture with the target of superpixel segmentation.
- A boundary-perceiving loss is designed to facilitate network to accurately identify boundary pixels, which is achieved by discriminating the features with different semantic labels around boundaries.
- State-of-the-art performance on four benchmarks including two natural datasets BSDS500 [4] and NYU [55] and

two medical benchmarks ISIC-2017 [9] and ACDC [28]. Besides, two stereo matching datasets, *i.e.* SceneFlow [48] and HR-VS [69], are further included to perform the downstream disparity matching task.

This manuscript makes following improvements on the basis of our conference version AINet [64]: We extend our AINet from a single implantation scheme to a hierarchical one (named AINet+), making the network better capture the pixel-superpixel relation, and promoting our performance one step further. To further verify the superiority of our methods, we additionally perform extensive experiments on two medical benchmarks, *i.e.*, ISIC-2017 [9], and ACDC [28]. Our AINet+ could outperform all of the competitive methods on these four datasets. What's more, to study the benefits of our AINet+ to the downstream task, we conduct experiments on the stereo matching on two popular benchmarks, SceneFlow [48] and HR-VS [69]. By equipping our AINet+, the performance of stereo matching model could get improved as expected.

In the following, we will first introduce the existing works related to this paper in section II. Section III would give some prior knowledge to ease the understanding of this paper. In section IV, we would elaborate the details of our proposed method. Experimental results on four benchmarks are presented in section V. Section VI gives the conclusions.

II. RELATED WORK

Superpixel segmentation seeks to group similar pixels for an image and is a fundamental problem in computer vision, extensive efforts have been dedicated to this task due to its important application for the downstream tasks. Hereinafter, we would revisit the existing works of superpixel segmentation and its application.

A. Superpixel Segmentation

Superpixel segmentation is a well-defined problem and has a long line of research [10], [26], [33], [46], [56], [61]. Traditional superpixel algorithms can be broadly classified into graph-based and clustering-based approaches. Graph-based methods consider the pixels as nodes and the edges as strength of connectivity between adjacent pixels, respectively. Consequently, the superpixel segmentation could be formulated as a graph-partitioning problem. Wide-used algorithms, Felzenszwalb and Huttenlocher (FH) [14] and the entropy rate superpixels (ERS) [42], belong to this category. Liu *et al.* [42] model the superpixel segmentation as a random walk on a graph, the authors utilize the entropy rate to make the superpixel compact and a balance term to encourage the clusters with the same size. On the other hand, clustering-based approaches utilize classic clustering techniques like k -means to compute the connectivity between the anchor pixels and its neighbors. Well-known methods in this category include SLIC [1], LSC [38], Manifold-SLIC [44] and SNIC [2]. Achanta *et al.* [1] adapt the k -means algorithm to superpixel segmentation, the designed SLIC method achieves good performance and efficiency simultaneously. Inspired by the success of deep learning techniques, recently, researchers attempt to utilize the deep neural network to learn the membership of each pixel to its surrounding

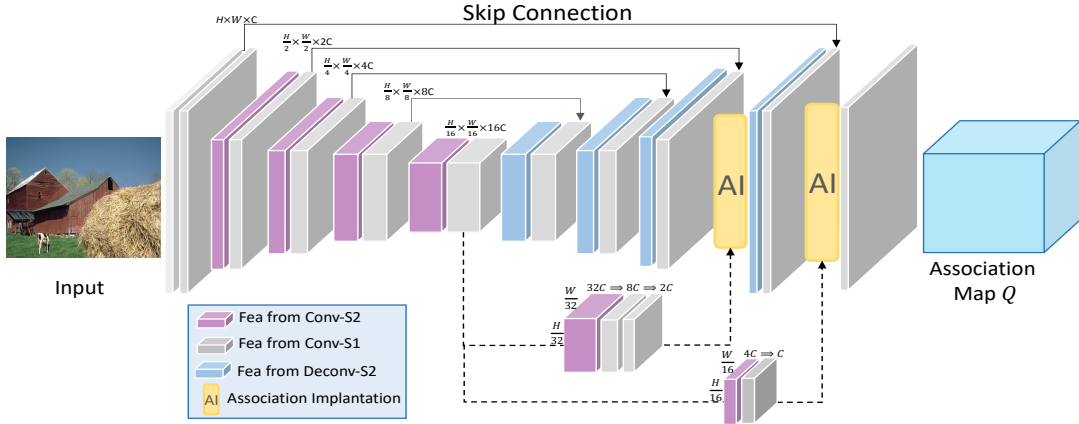


Fig. 2: The framework of our AINet+, where the conv/deconv means convolution/deconvolution, and conv-S# means convolution with stride #. The network takes an image as input and outputs the association map. Meanwhile, the superpixel embedding and pixel embedding are first obtained by the convolutions and then fed into the AI module to obtain the pixel-superpixel context. And the local patch loss is performed on the pixel-wise embeddings to boost the boundary precision. In AI module, the sampling interval is set to 16, and each block indicates a pixel or superpixel embedding.

grid cells. Tu *et al.* [60] attempt to learn deep features to benefit the superpixel segmentation, however, the overall architecture is still not differentiable. Jampani *et al.* [25] develop the first differentiable deep network motivated by the classic SLIC method, and Yang *et al.* [68] further simplify the framework and contribute a more efficient model. Zhu *et al.* [78] attempt to learn the superpixels in an unsupervised manner and propose to perform superpixel segmentation by a lifelong clustering problem.

B. Application of Superpixel

The pre-computed superpixel segmentation could be viewed as a type of weak label or prior knowledge to benefit many downstream tasks like image & video segmentation [7], [24], [63], [65], [72], object detection [37], [40], image super-resolution [71] and so on. The superpixels could be integrated into deep learning pipeline to provide guidance so that some important image properties (e.g., boundaries) could be better preserved [5], [18], [22], [36], [39], [58], [70]. For example, KwaK *et al.* [32] utilize the superpixel segmentation to perform a region-wise pooling to make the pooled feature have better semantic compactness. In [49], Cheng *et al.* consider the superpixel as pseudo label and attempt to boost the image segmentation by identifying more semantic boundary. Besides benefiting the image segmentation or feature pooling, superpixel also provides flexible ways to represent the image data. He *et al.* [21] convert 2D images patterns into 1D sequential representation, such a novel representation allows the deep network to explore the long-range context of the image. Gadde *et al.* [16] propose a bilateral inception module that propagates information between superpixels, the authors target on capturing more structure information with the guidance of superpixel. Liu *et al.* [43] learn the similarity between different superpixels, the developed framework could produce different grained segmentation regions by merging the superpixels according to the learned superpixel similarity. In [12], Dong *et al.* utilize the superpixel to guide the attention procedure and develop a robust adversarial attack framework.

Besides images, superpixel could also benefit the video-related tasks. For example, Wang *et al.* [62] treat the superpixel as a prior knowledge and integrate it into a video segmentation framework, the author use the superpixel to perform spatial and temporal pooling, which could provide good guidance for the video segmentation.

III. PRELIMINARIES

Before delving into the details of our method, we first introduce the framework of deep-learning based superpixel segmentation, which is also the fundamental theory of this paper. As illustrated in Fig. 1, the image I is partitioned into blocks using a regular size grid, and the grid cell is regarded as the initial superpixel seed. For each pixel p in image I , the superpixel segmentation aims at finding a mapping that assigns each pixel to one of its surrounding grids, *i.e.* 9 neighbors, just as shown in Fig. 1. Mathematically, deep-learning based method feeds the image $I \in \mathcal{R}^{H \times W \times 3}$ to convolution neural network and output an association map $Q \in \mathcal{R}^{H \times W \times 9}$, which indicates the probability of each pixel to its neighbor grids [25], [68]. Since there is no ground-truth for such an output, the supervision for network training is performed in an indirect fashion: the predicted association map Q serves as the intermediate variable to reconstruct the pixel-wise property $l(p)$ like semantic label, position vector, and so on. Consequently, there are two critical steps in training stage.

Step1: Estimate the superpixel property from the surrounding pixels:

$$h(s) = \frac{\sum_{p:s \in N_p} l(p) \cdot q(p, s)}{\sum_{p:s \in N_p} q(p, s)}. \quad (1)$$

Step2: Reconstruct the pixel property according to the superpixel neighbors:

$$l'(p) = \sum_{s \in N_p} h(s) \cdot q(p, s), \quad (2)$$

where the N_p is the set of adjacent superpixels of p , $q(p, s)$ indicates the probability of pixel p assigned to superpixel s .

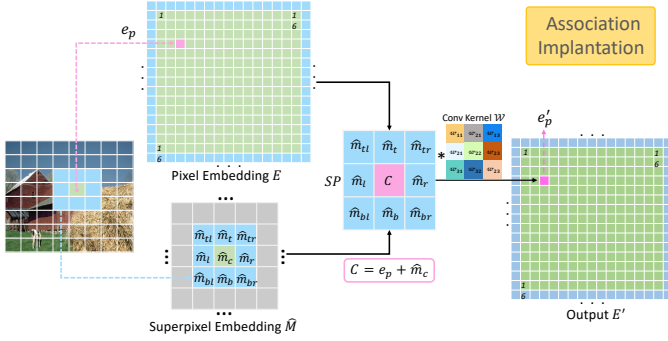


Fig. 3: Illustration of our Association Implantation Module (AI). We directly implant the surrounding grid features to the central pixels, such a design could allow the network to explicitly harvest the pixel-grid relation, which is the context exactly required by the superpixel segmentation.

The output $h(s)$ in step 1 is an average property for the initial superpixel s , which is estimated using the pixel association $q(p, s)$ to weight the pixel properties $l(p)$, the denominator $\sum_{p:s \in N_p} q(p, s)$ is used for normalization. In the next step, the pixel property $l'(p)$ is reconstructed in return using the association $q(p, s)$ to weighted sum the superpixel property estimation $h(s)$.

Thus, the training loss is to optimize the distance between the ground-truth property and the reconstructed one:

$$\mathcal{L}(Q) = \sum_p \text{dist}(l(p), l'(p)). \quad (3)$$

Following Yang's practice [68], the properties of pixel in this paper include the semantic label and the position vector, *i.e.*, two-dimension spatial coordinates, which are optimized by the cross-entropy loss and the \mathcal{L}_2 reconstruction loss, respectively.

IV. METHODOLOGY

An overview of our proposed AINet+ is shown in Fig. 2. In general, the overall architecture is an encoder-decoder style paradigm, the encoder module compresses the input image and outputs a feature map called superpixel embedding, whose pixels exactly encode the features of grid cells. Subsequently, the superpixel embedding is further fed into the decoder module to produce the association map. Meanwhile, the superpixel embedding and the pixel embedding in decoding stage are integrated to perform the association implantation, we also perform our association implantation on the second-last decoding layers to hierarchically capture the pixel-superpixel relation. The boundary-perceiving loss acts on the pixel embedding to help discriminate the pixels around boundary in hidden feature level. Hereinafter, we will first elaborate the details of our proposed AI module in subsection IV-A, in subsection IV-B, the hierarchical association implantation will be presented, and the designed boundary-perceiving loss would be introduced in subsection IV-C.

A. Association Implantation Module

To enable the network to explicitly perceive the relation between each pixel and its surrounding grid cells, this work

proposes an association implantation module to perform a direct interaction between the pixel and its neighbor grids. As shown in Fig. 3, we first obtain the embeddings of superpixels and pixels by the convolution network. Then, for each pixel embedding, the corresponding neighbor superpixel features are picked and implanted to its surrounding. Finally, a convolution with kernel size 3×3 is conducted on the expanded pixel embedding to achieve the knowledge propagation.

Formally, let $e_p \in \mathcal{R}^D$ be the embedding of pixel p from the pixel embedding $E \in \mathcal{R}^{H \times W \times D}$, which is obtained by the deep neural network as shown in Fig. 2. To obtain the embeddings of the grid cells, *i.e.*, superpixel embedding, we compress the input image by $\log_2 S$ times using multiple convolutions and max-pooling operations, where S is the sampling interval for the grid cell. For example, if the sampling interval is 16, then, we downsample the image 4 times. This would result in a feature map $M \in \mathcal{R}^{h \times w \times D'}$ whose pixels exactly encode the features of grid cells, where $h = H/S$, and $w = W/S$. To perform the implantation operation on the pixel embedding, we first adjust the channels of M using two 3×3 convolutions, producing a new map $\hat{M} \in \mathcal{R}^{h \times w \times D}$. Then, for the pixel p , we pick up its 9 adjacent superpixel embeddings from left to right and top down: $\{\hat{m}_{tl}, \hat{m}_t, \hat{m}_{tr}, \hat{m}_l, \hat{m}_c, \hat{m}_r, \hat{m}_{bl}, \hat{m}_b, \hat{m}_{br}\}$ from \hat{M} . To allow the network could explicitly capture the relation between pixel p and its neighbor grids, we directly implant the superpixel embeddings into the surrounding of the pixel p to provide pixel-superpixel context:

$$SP = \begin{bmatrix} \hat{m}_{tl} & \hat{m}_t & \hat{m}_{tr} \\ \hat{m}_l & \hat{m}_c + e_p & \hat{m}_r \\ \hat{m}_{bl} & \hat{m}_b & \hat{m}_{br} \end{bmatrix}. \quad (4)$$

It is worth noting that the pixels in the same initial grid would share the same surrounding superpixels, since they would degrade into one element in superpixel view. We then adopt a 3×3 convolution to adaptively distill information from the expanded window to benefit the subsequent association map inferring:

$$e'_p = \sum_{ij} SP_{ij} \times w_{ij} + b, \quad (5)$$

where w and b are the convolution weight and bias, respectively. We traverse all of the pixel embeddings in E and apply the operations in Eq. 4-5, thus, we could obtain a new pixel embedding E' whose elements capture the pixel-superpixel level context. In the following, the feature map E' is fed through a convolution layer to predict the association map Q .

As shown in Eq. 4-5, our AI module directly places the neighbor grid embeddings in the surrounding of the pixel to provide the context required by superpixel segmentation, which is an intuitive and reasonable solution. Comparing to the existing methods that use the stacked convolutions to accumulate the pixel-wise relation, the pixel-superpixel context captured by our AI module is more in line with the target of superpixel segmentation.

B. Towards Hierarchical Association Learning

Before predicting the membership of pixels, perceiving the pixel-grid relation in region level would ease the following

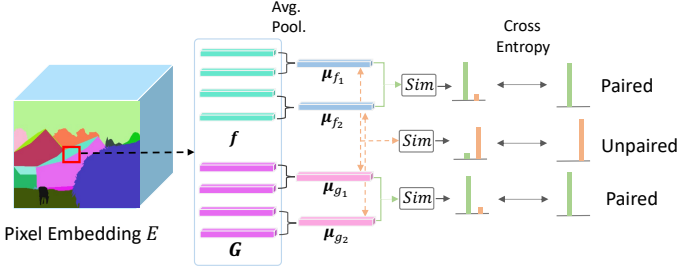


Fig. 4: Illustration of our Boundary-perceiving Loss (BPL). By performing a classification procedure on the boundary patches, we target at discriminating the boundary pixels in hidden feature level, which is achieved by enforcing the pixels with the same semantic label to be close while the different ones to be far away.

fine-grained assignment of pixels, this could be validated by many progressive and hierarchical frameworks [27], [31], [41]. Motivated by this, we enhance our network with a hierarchical association implantation. As shown in Fig. 2, we further apply our association implantation operation at the previous layer F of the pixel-embedding, the consecutive two AI modules enable the network to progressively harvest the pixel-grid relations.

The pixels in F encode a small 2×2 regions of the input image, to harvest its superpixel embedding M_{\downarrow} , we further down-sample the feature map M by a 3×3 convolution with stride 2, such that each pixel in M_{\downarrow} captures the features of a $2S \times 2S$ region of the input image. We next acquire \hat{M}_{\downarrow} by adjusting the channel dimension of M_{\downarrow} and perform the association implantation using F and \hat{M}_{\downarrow} . Different from the AI operation on the full resolution level, this association implantation is performed on the region level, which works together with the following AI module to form a hierarchical structure and enables the network to capture the pixel-superpixel relation in a coarse-to-fine manner.

C. Boundary-Perceiving Loss

Our boundary-perceiving loss is proposed to help the network appropriately assign the pixels around boundaries. As shown in Fig. 4, we first sample a series of patches with a certain size (5×5 , for example) around boundaries in the pixel embedding map, and then a classification procedure is conducted to improve the discrimination of the different semantic features.

Formally, let $E \in \mathcal{R}^{H \times W \times D}$ be the pixel-wise embedding map, since the ground-truth label is available during training stage, we could sample a local patch $B \in \mathcal{R}^{K \times K \times D}$ surrounding a boundary pixel from E . For the sake of simplification, the patch B only covers the pixels from two different semantic regions, that is, $B = \{f_1, \dots, f_m, g_1, \dots, g_n\}$, where $f, g \in \mathcal{R}^D, m + n = K^2$. Intuitively, we attempt to make the features in the same categories be closer, while the embeddings from different labels should be far away from each other. To this end, we evenly partition the features in the same categories



(a) Patch shuffle

(b) Random shift

Fig. 5: The illustrations for our patch jitter augmentation, patch shuffle and random shift. Color frames indicate the changed regions.

into two groups, f^1, f^2, g^1, g^2 , and employ a classification-based loss to enhance the discrimination of the features:

$$\mathcal{L}_B = -\frac{1}{2}(\log(\text{sim}(\mu_{f^1}, \mu_{f^2})) + \log(1 - \text{sim}(\mu_{f^1}, \mu_{g^1}))) - \frac{1}{2}(\log(\text{sim}(\mu_{g^1}, \mu_{g^2})) + \log(1 - \text{sim}(\mu_{f^2}, \mu_{g^2}))), \quad (6)$$

where the μ_{f^1} is the average representation for f^1 , and the function $\text{sim}(\cdot, \cdot)$ is the similarity measure for two vectors:

$$\mu_{f^1} = \frac{1}{|f^1|} \sum_{f \in f^1} f, \quad (7)$$

$$\text{sim}(f, g) = \frac{2}{1 + \exp(\|f - g\|_1)}, \quad (8)$$

Taking all of the sampled patches \mathcal{B} into consideration, our full boundary-perceiving loss is formulated as follow:

$$\mathcal{L}_B = \frac{1}{|\mathcal{B}|} \sum_{B \in \mathcal{B}} \mathcal{L}_B. \quad (9)$$

Overall, the full losses for our network training comprise three components, *i.e.*, cross-entropy (CE) and \mathcal{L}_2 reconstruction losses for the semantic label and position vector according to the Eq. 3, and our boundary-perceiving loss:

$$\mathcal{L} = \sum_p CE(l'_s(p), l_s(p)) + \lambda \|p - p'\|_2^2 + \alpha \mathcal{L}_B \quad (10)$$

where $l'_s(p)$ is the reconstructed semantic label from the predicted association map Q and the ground-truth label $l_s(p)$ according to Eq. 1-2, and λ, α are two trade-off weights.

V. EXPERIMENTS

Datasets. We conduct experiments on four public benchmarks, **BSDS500** [4], **NYUv2** [55], **ISIC-2017** [9], and **ACDC** [28] to evaluate the effectiveness of our method. BSDS500 comprises 200 training, 100 validation and 200 test images, and each image is annotated by multiple semantic labels from different experts. To make a fair comparison, we follow previous works [25], [60], [68] and treat each annotation as an individual sample. Consequently, 1,087 training, 546 validation samples and 1,063 testing samples could be obtained. NYUv2 is an indoor scene understanding dataset and contains 1,449 images with object instance labels. To evaluate the superpixel methods, Stutz *et al.* [56] remove the unlabelled regions near the boundary and collect a subset of 400 test images with

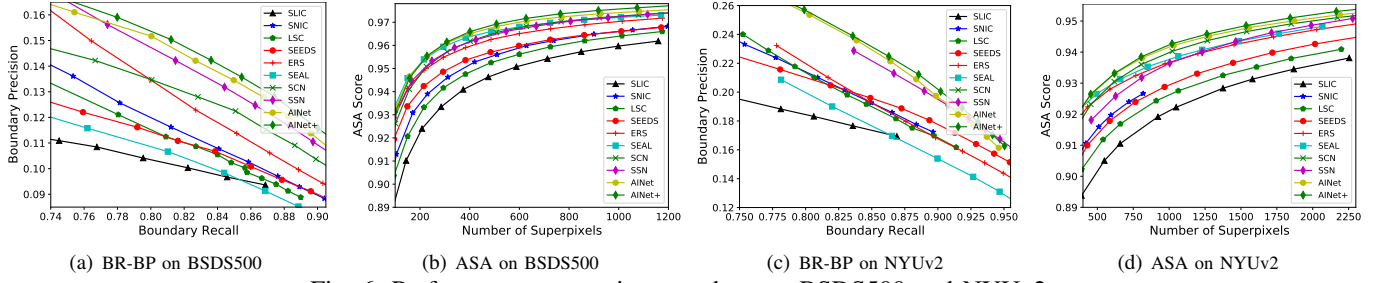


Fig. 6: Performance comparison on datasets BSDS500 and NYUv2.

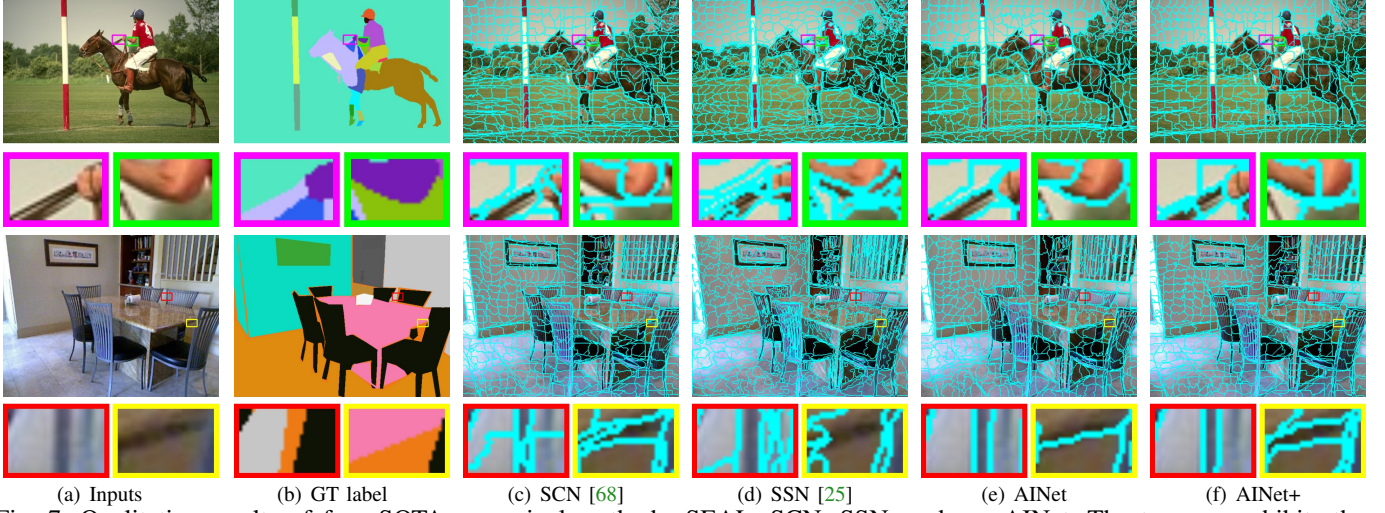


Fig. 7: Qualitative results of four SOTA superpixel methods, SEAL, SCN, SSN, and our AINet. The top row exhibits the results from BSDS500 dataset, while the bottom row shows the superpixels on NYUv2 dataset.

size 608×448 for superpixel evaluation. To further validate the effectiveness of our proposed model, we also additionally introduce two medical datasets, **ISIC-2017** [9] and **ACDC** [28], for performance evaluation. The ISIC-2017 dataset contains skin lesion images and the corresponding manually annotated lesion delineations belonging to four diagnoses: melanoma, seborrheic, keratosis, and benign nevi. Following the official split, we use 2,000, 150, and 600 for training, validation and testing, respectively. ACDC contains 100 cine magnetic resonance (MR) exams covering well defined pathologies: dilated cardiomyopathy, hypertrophic cardiomyopathy, myocardial infarction with altered left ventricular ejection fraction and abnormal right ventricle, and also include normal subjects. Each exam only contains acquisitions at the diastolic and systolic phases. We use 75 exams for training and 10 exams for validation, the left 15 exams is used for testing.

Following Yang’s practice [68], we conduct a standard train and test pipeline on the BSDS500 dataset. On the subject of NYUv2 dataset, we directly apply the model trained on BSDS500 and report the performance on the 400 tests to evaluate the generality of the model. As for the two medical datasets, since their samples have considerable difference, therefore, we train and test the models on their respective data splits.

Augmentation via Patch Jitter. To further improve the performance and enhance the generality of our model, we propose to augment the data by jittering the image patches.

Specifically, the proposed patch jitter augmentation comprises two components, *i.e.*, patch shuffle and random shift. Fig. 5 gives one example for each type of augmentation.

Patch Shuffle Assume S is the superpixel sampling interval, for an image, we randomly pick up two patches $\{U, V\}$ with shape $S \times S$ and exchange their positions. The corresponding label patches are also exchanged accordingly. After that, we randomly select one cell from $\{U, V\}$, and 1) keep it unchanged with probability 0.75 or 2) replace it using a random patch from normal distribution with probability 0.25. To maintain the consistency between image and label, we expand the label dimension and assign the random patch with the new label.

Random Shift The proposed random shift augmentation could be applied in two directions, *i.e.*, horizontal and vertical. For convenience sake, we take the horizontal random shift as an example to elaborate the process. we first random sample a cell C with shape $S \times L$, where $L = \text{rand_int}(S, W)$, then the sampled cell C is translated by a random offset $o = \text{rand_int}(0, S)$. The translation could be conducted along two directions, *i.e.*, the left and the right. Consequently, two new patches could be produced: $C_l = [C_{:,o}, C_{:,o}]$ for left translation and $C_r = [C_{:,-o}, C_{:,-o}]$ for right translation, where $[\cdot, \cdot]$ means concatenating along width. To further extend the image pattern, we also employ the same random patch trick in patch shuffle, that is, the $C_{:,o}$ or the $C_{:,-o}$ could be replaced by a random patch with probability 0.25. Finally,

the augmentation is done by random replacing the C with C_l or C_r . Analogously, the augmentation along vertical direction could be done similarly. In our experiments, horizontal and vertical augmentation is randomly conducted.

The patch jitter augmentation is repeated 2 times during training, and SCN [68] is adopted as our baseline method in our experiments.

Implementation Details. In training stage, the image is randomly cropped to 256×256 as input, and the network is trained using the adam optimizer [30] for 4k iterations with batch size 16. The learning rate starts with $8e-5$ and is discounted by 0.5 for every 2K iterations. The sampling interval is fixed as 16, consequently, the encoder part employs 4 convolution&pooling operations to get the superpixel embedding M with shape $14 \times 14 \times 256$. The following decoder module produces the pixel embedding with shape $256 \times 256 \times 16$ using 4 convolution&deconvolution operations. Then, the channels of superpixel embedding are first compressed by two convolution layers: $256 \Rightarrow 64 \Rightarrow 16$, then our AI module is performed. Our AI module could be effectively implemented by a repeat and mask operation. Specifically, each pixel embedding in E is repeated to form a $3 \times 3 \times D$ cubic, thus, the expanded E (marked as E^*) is with shape $(3H) \times (3W) \times D$. Next, we slide a 3×3 window on Sp embedding and repeat the overall 3×3 patch by 16 \times 16 times, since the pixels in the same grid share the 9 neighbor grids (see Fig. 1), consequently, the shape of the expanded Sp embedding (marked as M^*) is also $(3H) \times (3W) \times D$. A mask G is pre-defined by repeating 3×3 matrix $[0,0,0; 0,1,0; 0,0,0]$ $H \times W$ times. Then, the implantation operation (Eq.5) is implemented: $\hat{F} = G \odot E^* + M^*$. Finally, a 3×3 conv with stride 3 is applied on \hat{F} to get the output E' , which is fed forward to the next layer.

To perform the association module on the second-last layer, we first down-sample the bottleneck feature M by a 3×3 convolution with stride 2, and adjust its channels by two convolution layers: $512 \Rightarrow 128 \Rightarrow 32$, and the AI module is analogously performed. The boundary-perceiving loss also acts on the pixel embedding, where the patch size is set to 5, *i.e.*, $K = 5$. In the following, two convolution layers are stacked to predict the association map Q with shape $256 \times 256 \times 9$. In our conference version, the input resolution is 208×208 , we enlarge the resolution as 256 in this work to enable the downsampling to appropriately go one more step, such that the association implantation could be performed on the second-last layer. But it is worthy noting that simply enlarging the resolution did not improve the performance in our experiments, therefore, the performance gain is not from the larger resolution. In our practice, simultaneously equipping the boundary-perceiving loss and AI Module could not make the performance step further, therefore, we first train the network using the first two items in Eq. 10 for 3K iterations, and use the boundary-perceiving loss to finetune 1K. Following Yang’s practice [68], the weight of position reconstruction loss is set to 0.003/16, while the weight for our boundary-perceiving loss is fixed to 0.5, *i.e.*, $\lambda = 0.003/16, \alpha = 0.5$. In testing, we employ the same strategy as [68] to produce

varying numbers of superpixels. For example, if we want to produce 400 superpixels, the image would be resized to 320×320 .

Several methods are considered for performance comparison, including classic methods, SLIC [1], LSC [38], ERS [42], SEEDS [11], SNIC [2] and deep learning-based methods, SEAL [60], SSN [25], SCN [68]. We simply use the OpenCV implementation for methods SLIC, LSC and SEEDS. For other methods, we use the official implementations with the recommended parameters from the authors. AINet [64] is the conference version of our method, while AINet+ refers to AINet equipped with the hierarchical association implantation, *i.e.*, the method proposed in this paper.

Evaluation Metrics. We use three popular metrics including achievable segmentation accuracy (ASA), boundary recall (BR) and boundary precision (BP) to evaluate the performance of superpixel. ASA score studies the upper bound on the achievable segmentation accuracy using superpixel as pre-processing step, while BR and BP focus on accessing how well the superpixel model could identify the semantic boundaries. The higher value of these metrics indicates better superpixel segmentation performance.

A. Comparison with the state-of-the-art methods

Fig. 6 reports the quantitative comparison results on BSDS500 and NYUv2 test sets. As indicated in Fig. 6, our AINet+ attains the best ASA score and BR-BP on both datasets. With the help of deep convolution networks, the methods, SEAL, SCN, SSN, AINet and AINet+ could achieve superior or comparable performance against the traditional superpixel algorithms, and our AINet and AINet+ are the top 2 models among them. From Fig. 6 (a)-(b), the AINet could surpass the traditional methods by a large margin on BSDS500 dataset. By harvesting the pixel-sueprpixel level context and highlighting the boundaries, AINet could also outperform the deep methods SEAL, SCN and SSN. The hierarchical AI module further boosts the performance, our AINet+ achieves the most outstanding performance. Fig. 6 (c)-(d) shows the performance when adapting to the NYUv2 test set, we can observe that the AINet and AINet+ also shows better generality. Although the BR-BP is comparable with the SCN and SSN, ASA scores of AINet and AINet+ are more outstanding than all of the competitive methods.

To further evaluate our method, we also conduct experiments on two widely-used medical benchmarks, *i.e.*, ISIC-2017 [9] and ACDC [28], Fig. 8 exhibits the performance comparison on these two benchmarks. From Fig. 8, we can see that the superiority of our AINet and AINet+ are clearer, both AINet and AINet+ could surpass all competing methods by a large margin on both the BR-BP and ASA score. Comparing to AINet, our AINet+ could attain better results.

Fig. 7 and Fig. 9 subsequently show the qualitative results of four state-of-the-art methods on dataset BSDS500, NYUv2, ISIC-2017 and ACDC, comparing to the competitive methods, the boundaries of our results are more accurate and clearer, which intuitively shows the superiority of our method.

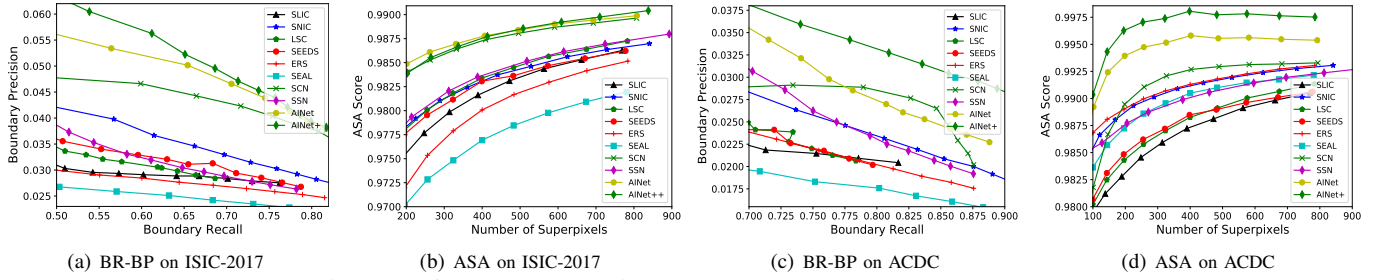


Fig. 8: Performance comparison on datasets ISIC-2017 and ACDC.

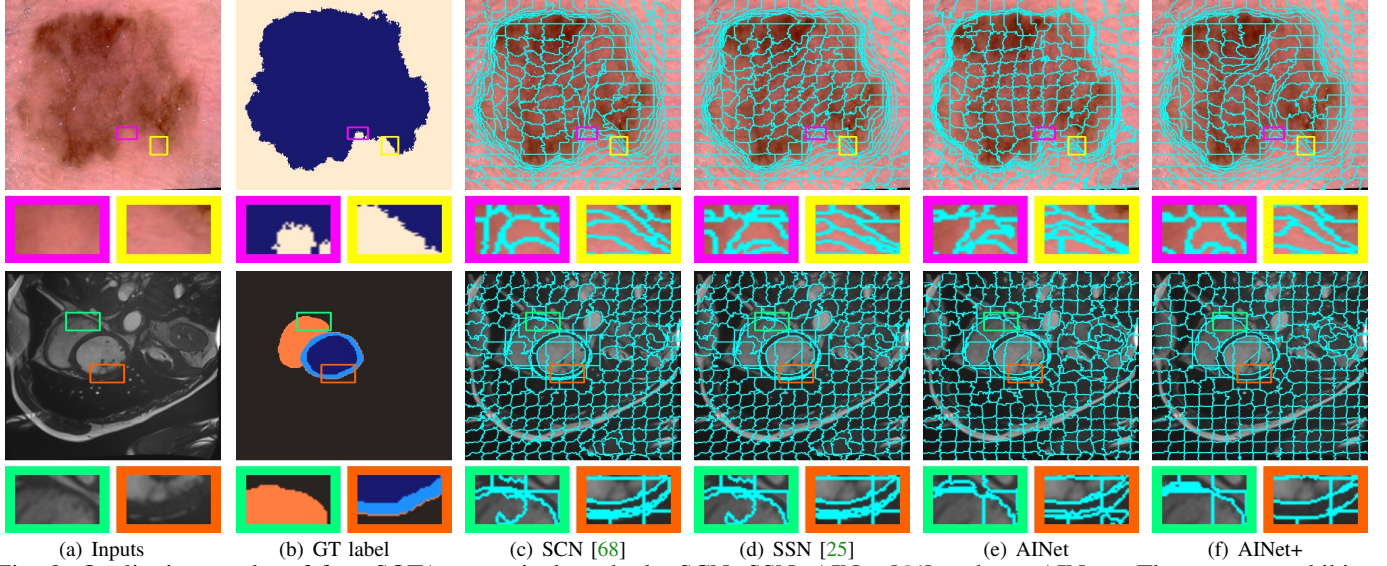


Fig. 9: Qualitative results of four SOTA superpixel methods, SCN, SSN, AINet [64] and our AINet+. The top row exhibits the results from ISIC-2017 dataset, while the bottom row shows the superpixels on ACDC dataset.

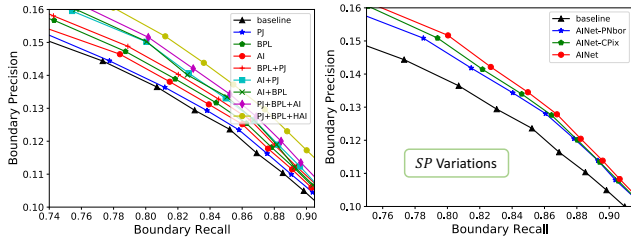


Fig. 10: Ablation study on BSDS500, where the AI, BPL, PJ and HAI refer to the association implantation, boundary perceiving loss, patch jitter and the hierarchical association implantation module. The left figure shows the contributions of each component in our system, while the right one discusses two variations of SP (Eq. 4).

B. Ablation Study

To validate the respective contributions of our proposed modules including the data augmentation trick, AI module, and the boundary-perceiving loss, we conduct ablation study on BSDS500 dataset to thoroughly study their effectiveness. The left figure in Fig. 10 reports the performances of all methods, where the BPL means the boundary-perceiving loss, and BPL+PJ stands for the baseline simultaneously equipped with the boundary-perceiving loss and the patch jitter augmentation. From Fig. 10, we can observe that individually

applying the three modules on the baseline method could all boost the performance, and the boundary-perceiving loss could contribute the most performance gains. The combination of the patch jitter augmentation and the BPL or AI Module could make the performance step further, and the AI module equipped with the data augmentation achieves better performance. When simultaneously employing the three modules, the performance gets further improved. By equipping the hierarchical AI operation, we could harvest the best BR-BP.

Besides, we also give a discussion for two alternative choices of SP (Eq. 4): a greedy version of SP that further adds the neighbor pixels to the corresponding surrounding superpixels like the central position, for example, \hat{m}_t is replaced by $\hat{m}_t + e_t$; And a simplified version that ignoring the central superpixel, i.e., $\hat{m}_c + e_p$ changes to e_p . The models with the above two versions of SP are marked as AINet-PNbor and AINet-CPix, respectively. The right figure of Fig. 10 shows the results, we can observe that AINet-PNbor and AINet-CPix could both surpass the baseline but perform a litter worse than AINet. By summing the neighbor pixels, the AINet-PNbor could integrate the pixel-wise relation, on the other hand, the sum operation would also reduce the force of superpixel embedding, which would conspire against capturing the pixel-superpixel context. For AINet-CPix, the excluded \hat{m}_c is also one of the neighbor superpixels, directly abandoning \hat{m}_c would fail to explicitly perceive the relation between pixel e_p and

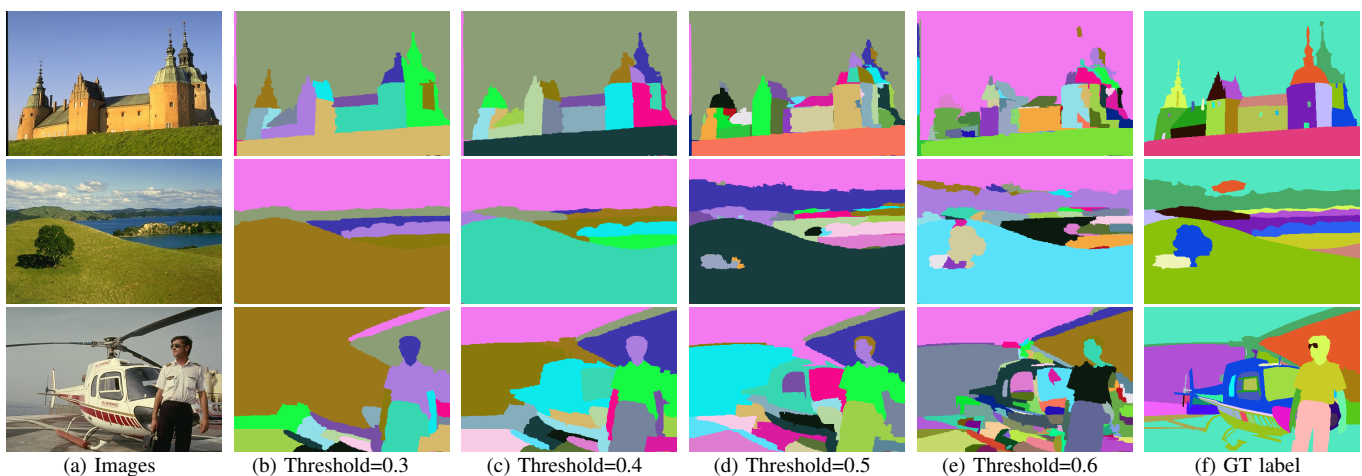
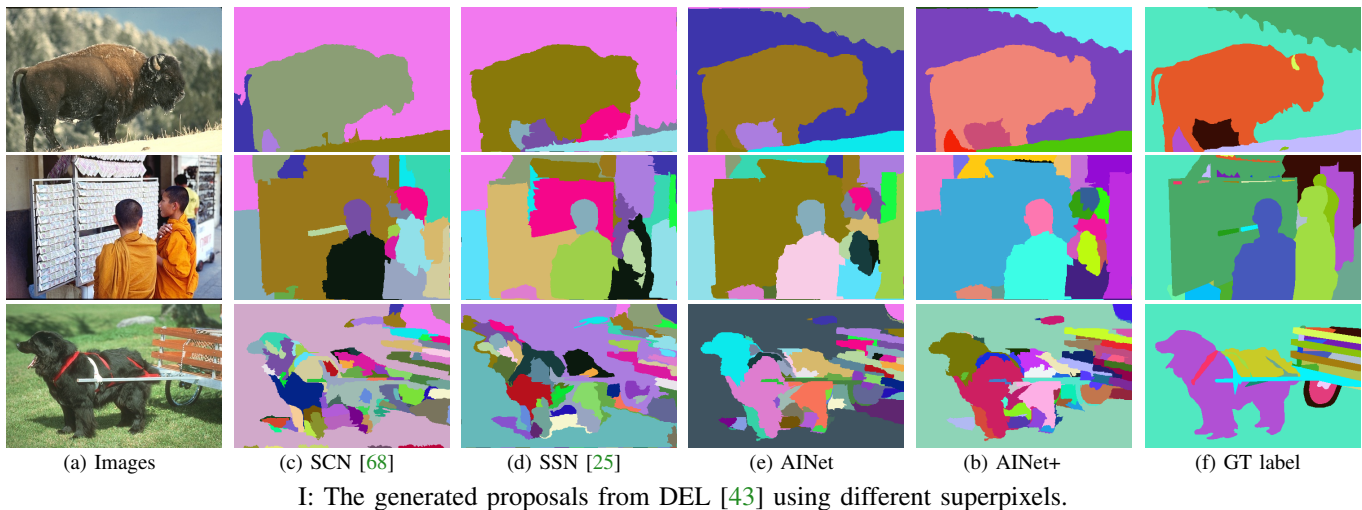


Fig. 11: Qualitative proposals from DEL [43] using different superpixels (I), and the results of DEL [43] with our superpixel using different thresholds (II), where threshold=0.3 mean merging the adjacent superpixels if their similarity is above 0.3.

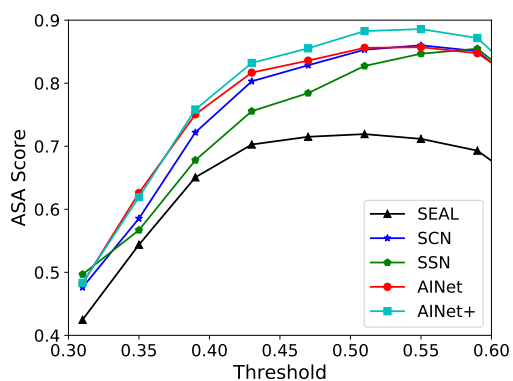


Fig. 12: The ASA scores of four state-of-the-art methods on object proposal generation.

central superpixel \hat{m}_c . Consequently, the above two variations of SP are both not effective to capture the super context.

C. Inference Efficiency

Besides the performance, the inference speed is also a concerned aspect. Therefore, we conduct experiments on

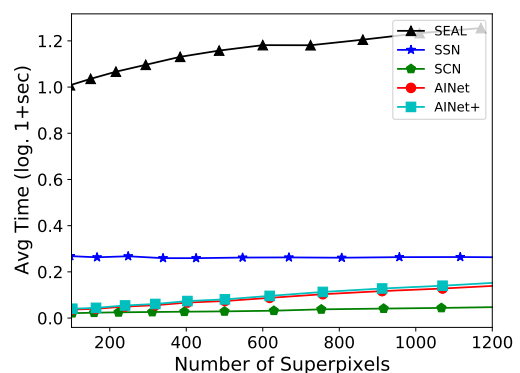


Fig. 13: The average time costs of four deep learning based methods w.r.t number of superpixels. The runtime is added with 1 and scaled by logarithmic to show positive values and a clear tendency.

BSDS500 dataset to investigate the inference efficiency of five deep learning-based methods. To make a fair comparison, we only count the time of network inference and post-processing steps (if available). All methods run on the same workstation

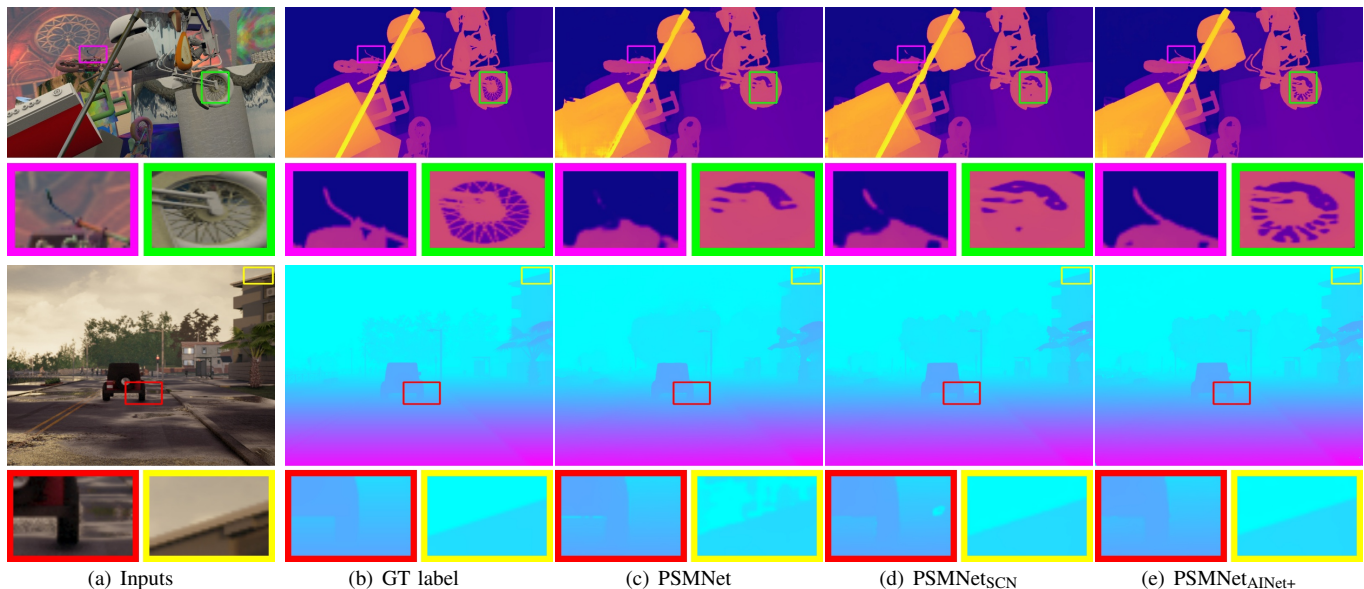


Fig. 14: Qualitative disparity predictions of three methods. The top row exhibits the results from SceneFlow dataset, while the bottom row shows the prediction on HR-VS dataset. By integrating the superpixels into the baseline PSM model, the results could be improved, and the PSM with our AINet+ outperforms the other approaches.

with NVIDIA 1080Ti GPU and Intel E5 CPU.

The time costs of five deep learning-based methods, SEAL, SCN, SSN, AINet and AINet+ are reported in Fig. 13. The method SCN achieves the best inference efficiency due to its simple architecture, while our AINet introduces more layers and operations, consequently, the inference is slightly slower than the SCN. The superpixel segmentation of SEAL and SSN is much complex comparing to the SCN and our AINet, SEAL needs first output the learned deep features and then feed them to a traditional algorithm to conduct superpixel segmentation, and SSN further performs the K -means iteration after obtaining the pixel affinity. As a result, SEAL and SSN both cost much more time in inference stage. Although the SCN is faster, its performance is not that satisfactory. AINet could attain much better performance at the acceptable cost of inference time. Comparing to AINet, AINet+ further include one more AI module, consequently, its inference is slightly slower than AINet. Considering the performance gain, the inference cost is acceptable.

D. Application on Object Proposal Generation

Image annotation is one of the important application scenarios for superpixels, since it could identify the semantic boundaries and provide the contours of many semantic regions. To generate the object proposals, Liu *et al.* [43] propose a model named DEL, they first estimate the similarities between superpixels and merge them according to a certain threshold, by which the proposed method could flexibly control the grain size of object proposal. In this subsection, we study the quality of object proposals based on the superpixels from different methods to further investigate the superiority of our methods. Specifically, we first feed the superpixels from five state-of-the-art methods, SEAL, SCN, SSN, AINet and AINet+ to the framework of [43], according to the estimated similarities, we

merge the superpixels according to a threshold to produce object proposals. To evaluate the performance, we use the ASA score to measure how well the produced object proposals cover the ground-truth labels:

$$ASA(O, G) = \frac{1}{N} \sum_{O_k} \max_k \{|O_k \cap G_k|\}, \quad (11)$$

where N is the number of generated object proposal O , and G is the ground-truth semantic label.

The performance of all methods is reported in Fig. 12, from which we can observe that the average performance of our AINet and AINet+ is more outstanding than other deep learning-based methods. The models AINet+, AINet, SCN and SSN could be trained in an end-to-end manner, and all perform better than the SEAL, among them, our AINet+ is the most outstanding method. Fig. 11 I shows three results of DEL [43] with the superpixels from four methods, different thresholds are used to produce varied size proposals: the adjacent superpixels would be merged if their similarity is above the threshold, which means that higher value would produce finer object proposals. As shown in Fig. 11 I, our AINet and AINet+ could generate more satisfactory object proposals comparing to the competing methods, which validates the effectiveness of our proposed methods. Fig. 11 II exhibits the results using the superpixels of our AINet with different thresholds, varying sizes of generated object proposals could be generated by adjusting the threshold.

E. Application on Stereo Matching

Besides directly applying for dense annotation task, superpixels could also be integrated into many deep frameworks to provide some guidance, such that some performance gains could be obtained. In this subsection, we conduct experiments

Method	PSMNet [6]	PSMNet _{SCN}	PSMNet _{AINet}	PSMNet _{AINet+}
SceneFlow	1.04	0.93	0.89	0.84
HR-VS	3.83	2.77	2.23	2.02

TABLE I: The End-point-error (EPE) of four methods on SceneFlow and HR-VS datasets.

to further study the effectiveness of our superpixels on stereo matching task.

Stereo matching seeks to build pixel correspondences between a pair of rectified images. Most recent works promote the performance at the cost of high computation and memory cost [6], [8], [80]. Liu *et al.* [68] propose to integrate the superpixel segmentation network for memory-saving. Specifically, the input image I is first fed into the superpixel segmentation network to acquire the association map Q , then I is down-sampled using Eq. 1 and fed forward the stereo matching network for disparity prediction. Finally, the full resolution disparity is obtained by upsampling the disparity using Eq. 2, we use the disparity regression and superpixel losses to joint train the stereo matching and the superpixel networks. More detailed configuration could be found in [68].

We conduct experiments on two benchmarks of stereo matching, *i.e.*, SceneFlow [48] and HR-VS [69]. To make a fair comparison, the experiments on these two datasets follow the same configuration of SCN. We take PSMNet as our baseline method. The End-point-error (EPE) is used for performance evaluation, and the results are reported in Table I, where PSMNet_{SCN} means the PSMNet equipped with the superpixel network SCN. From Table I, we can find that the superpixel network could help improve the stereo matching. Comparing to the baseline model PSMNet, introducing the superpixels from SCN, AINet and AINet+ could all boost the performance. For example, when the SCN network is applied to the PSMNet, the EPE on SceneFlow could be improved from 1.04 to 0.93, the AINet and AINet+ make the performance step further, and the PSMNet equipped with our AINet+ achieves the best results. Fig. 14 shows the visualization of three methods, from which we could intuitively observe the superiority of our method.

VI. CONCLUSION

We have presented an association implantation network for superpixel segmentation task. A novel association implantation module is proposed to provide the consistent pixel-superpixel level context for superpixel segmentation task, we plug the association implantation operation in multiple layers to further boost the performance. By applying our AI module to multi-layers, the model could obtain the hierarchical pixel-superpixel context. Such a design makes the network more effectively infer the association map, bringing more performance gains. To pursue better boundary precision, a boundary-perceiving loss is designed to improve the discrimination of pixels around boundaries in hidden feature level, and a data augmentation named patch jitter is developed to further improve the performance. Experiments on two popular benchmarks show that the proposed method could achieve state-of-the-art performance with good generalizability. What's more, the produced superpixels by our method could also perform well when applied

to the object proposal generation and stereo matching tasks. In the future, we will continue to study the application of superpixel on segmentation task.

REFERENCES

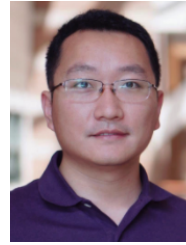
- [1] Radhakrishna Achanta, Appu Shaji, Kevin Smith, Aurélien Lucchi, Pascal Fua, and Sabine Süsstrunk. SLIC superpixels compared to state-of-the-art superpixel methods. *IEEE Trans. Pattern Anal. Mach. Intell. (TPAMI)*, 34(11):2274–2282, 2012. 1, 2, 7
- [2] Radhakrishna Achanta and Sabine Süsstrunk. Superpixels and polygons using simple non-iterative clustering. In *IEEE Conference on Computer Vision and Pattern Recognition (CVPR)*, pages 4895–4904, 2017. 1, 2, 7
- [3] Roberto Amoroso, Matteo Tomei, Lorenzo Baraldi, and Rita Cucchiara. Superpixel positional encoding to improve vit-based semantic segmentation models. In *34th British Machine Vision Conference 2023, BMVC 2023, Aberdeen, UK, November 20-24, 2023*, page 623. BMVA Press, 2023. 1
- [4] Pablo Arbelaez, Michael Maire, Charless C. Fowlkes, and Jitendra Malik. Contour detection and hierarchical thermal image segmentation. *IEEE Trans. Pattern Anal. Mach. Intell. (TPAMI)*, 33(5):898–916, 2011. 2, 5
- [5] András Bódis-Szomorú, Hayko Riemenschneider, and Luc Van Gool. Superpixel meshes for fast edge-preserving surface reconstruction. In *IEEE Conference on Computer Vision and Pattern Recognition (CVPR)*, pages 2011–2020, June 2015. 3
- [6] Jia-Ren Chang and Yong-Sheng Chen. Pyramid stereo matching network. In *IEEE Conference on Computer Vision and Pattern Recognition (CVPR)*, pages 5410–5418, 2018. 11
- [7] Zixuan Chen, Huajun Zhou, Jianhuang Lai, Lingxiao Yang, and Xiaohua Xie. Contour-aware loss: Boundary-aware learning for salient object segmentation. *IEEE Trans. Image Processing (TIP)*, 30:431–443, 2021. 3
- [8] Xinjing Cheng, Peng Wang, and Ruigang Yang. Learning depth with convolutional spatial propagation network. *IEEE Trans. Pattern Anal. Mach. Intell. (TPAMI)*, 42(10):2361–2379, 2020. 11
- [9] Noel C. F. Codella, David A. Gutman, M. Emre Celebi, Brian Helba, Michael A. Marchetti, Stephen W. Dusza, Aadi Kallou, Konstantinos Liopyris, Nabin K. Mishra, Harald Kittler, and Allan Halpern. Skin lesion analysis toward melanoma detection: A challenge at the 2017 international symposium on biomedical imaging (isbi), hosted by the international skin imaging collaboration (ISIC). In *ISBI 2018*, pages 168–172. IEEE, 2018. 2, 5, 6, 7
- [10] Dorin Comaniciu and Peter Meer. Mean shift: A robust approach toward feature space analysis. *IEEE Trans. Pattern Anal. Mach. Intell. (TPAMI)*, 24(5):603–619, 2002. 2
- [11] Michael Van den Bergh, Xavier Boix, Gemma Roig, and Luc Van Gool. SEEDS: superpixels extracted via energy-driven sampling. *Int. J. Comput. Vis. (IJCV)*, 111(3):298–314, 2015. 7
- [12] Xiaoyi Dong, Jiangfan Han, Dongdong Chen, Jiayang Liu, Huan Yu, Zehua Ma, Hongsheng Li, Xiaogang Wang, Weiming Zhang, and Nenghai Yu. Robust superpixel-guided attentional adversarial attack. In *IEEE Conference on Computer Vision and Pattern Recognition (CVPR)*, pages 12892–12901, 2020. 1, 3
- [13] Fadi Dornaika and Danyang Sun. Lgcoamix: Local and global context-and-object-part-aware superpixel-based data augmentation for deep visual recognition. *IEEE Trans. Image Process.*, 33:205–215, 2024. 1
- [14] Pedro F. Felzenszwalb and Daniel P. Huttenlocher. Efficient graph-based image segmentation. *Int. J. Comput. Vis. (IJCV)*, 59(2):167–181, 2004. 2
- [15] Raghudeep Gadde, Varun Jampani, Martin Kiefel, Daniel Kappler, and Peter V. Gehler. Superpixel convolutional networks using bilateral inceptions. In *European Conference on Computer Vision (ECCV)*, pages 597–613, 2016. 1
- [16] Raghudeep Gadde, Varun Jampani, Martin Kiefel, Daniel Kappler, and Peter V. Gehler. Superpixel convolutional networks using bilateral inceptions. In *European Conference on Computer Vision (ECCV)*, pages 597–613, 2016. 3
- [17] Yuan Gao, Zilei Wang, Yixin Zhang, and Bohai Tu. Efficient active domain adaptation for semantic segmentation by selecting information-rich superpixels. In Ales Leonardis, Elisa Ricci, Stefan Roth, Olga Russakovsky, Torsten Sattler, and Gül Varol, editors, *Computer Vision - ECCV 2024 - 18th European Conference, Milan, Italy, September 29-October 4, 2024, Proceedings, Part XXXIV*, volume 15092 of *Lecture Notes in Computer Science*, pages 405–421. Springer, 2024. 1
- [18] Utkarsh Gaur and B. S. Manjunath. Superpixel embedding network. *IEEE Trans. Image Processing (TIP)*, 29:3199–3212, 2020. 3

- [19] Shengfeng He, Rynson W. H. Lau, Wenxi Liu, Zhe Huang, and Qingxiong Yang. Supercnn: A superpixelwise convolutional neural network for salient object detection. *Int. J. Comput. Vis. (IJCV)*, 115(3):330–344, 2015. **1**
- [20] Shengfeng He, Rynson W. H. Lau, Wenxi Liu, Zhe Huang, and Qingxiong Yang. Supercnn: A superpixelwise convolutional neural network for salient object detection. *Int. J. Comput. Vis. (IJCV)*, 115(3):330–344, 2015. **1**
- [21] Shengfeng He, Rynson W. H. Lau, Wenxi Liu, Zhe Huang, and Qingxiong Yang. Supercnn: A superpixelwise convolutional neural network for salient object detection. *Int. J. Comput. Vis. (IJCV)*, 115(3):330–344, 2015. **3**
- [22] Teng Hu, Ran Yi, Baihong Qian, Jiangning Zhang, Paul L. Rosin, and Yu-Kun Lai. Supersvg: Superpixel-based scalable vector graphics synthesis. In *IEEE/CVF Conference on Computer Vision and Pattern Recognition, CVPR 2024, Seattle, WA, USA, June 16–22, 2024*, pages 24892–24901. IEEE, 2024. **3**
- [23] Yinlin Hu, Rui Song, Yunsong Li, Peng Rao, and Yangli Wang. Highly accurate optical flow estimation on superpixel tree. *Image Vis. Comput.*, 52:167–177, 2016. **1**
- [24] Zilong Huang, Yunchao Wei, Xinggong Wang, Humphrey Shi, Wenyu Liu, and Thomas S. Huang. Alignseg: Feature-aligned segmentation networks. *IEEE Trans. Pattern Anal. Mach. Intell. (TPAMI)*, pages 1–1, 2021. **3**
- [25] Varun Jampani, Deqing Sun, Ming-Yu Liu, Ming-Hsuan Yang, and Jan Kautz. Superpixel sampling networks. In *European Conference on Computer Vision (ECCV)*, volume 11211, pages 363–380, 2018. **1, 3, 5, 6, 7, 8, 9**
- [26] Xuejing Kang, Lei Zhu, and Anlong Ming. Dynamic random walk for superpixel segmentation. *IEEE Trans. Image Processing (TIP)*, 29:3871–3884, 2020. **2**
- [27] Tero Karras, Timo Aila, Samuli Laine, and Jaakko Lehtinen. Progressive growing of gans for improved quality, stability, and variation. In *International Conference on Learning Representations (ICLR)*, 2018. **5**
- [28] Hoel Kervadec, Jose Dolz, Meng Tang, Eric Granger, Yuri Boykov, and Ismail Ben Ayed. Constrained-cnn losses for weakly supervised segmentation. *Medical Image Anal.*, 54:88–99, 2019. **2, 5, 6, 7**
- [29] Hoyoung Kim, Minhyeon Oh, Sehyun Hwang, Suha Kwak, and Jungseul Ok. Adaptive superpixel for active learning in semantic segmentation. In *IEEE/CVF International Conference on Computer Vision, ICCV 2023, Paris, France, October 1–6, 2023*, pages 943–953. IEEE, 2023. **1**
- [30] Diederik P. Kingma and Jimmy Ba. Adam: A method for stochastic optimization. In *International Conference on Learning Representations (ICLR)*, 2015. **7**
- [31] Sumith Kulal, Jiayuan Mao, Alex Aiken, and Jiajun Wu. Hierarchical motion understanding via motion programs. In *IEEE Conference on Computer Vision and Pattern Recognition (CVPR)*, pages 6568–6576. Computer Vision Foundation / IEEE, 2021. **5**
- [32] Suha Kwak, Seunghoon Hong, and Bohyung Han. Weakly supervised semantic segmentation using superpixel pooling network. In *AAAI Conference on Artificial Intelligence (AAAI)*, pages 4111–4117, 2017. **1, 3**
- [33] Alex Levinshtein, Adrian Stere, Kiriakos N. Kutulakos, David J. Fleet, Sven J. Dickinson, and Kaleem Siddiqi. Turbopixels: Fast superpixels using geometric flows. *IEEE Trans. Pattern Anal. Mach. Intell. (TPAMI)*, 31(12):2290–2297, 2009. **2**
- [34] Hua Li, Sam Kwong, Chuanbo Chen, Yuheng Jia, and Runmin Cong. Superpixel segmentation based on square-wise asymmetric partition and structural approximation. *IEEE Trans. Multimed.*, 21(10):2625–2637, 2019. **1**
- [35] Hua Li, Junyan Liang, Ruiqi Wu, Runmin Cong, Wenhui Wu, and Sam Tak-Wu Kwong. Stereo superpixel segmentation via decoupled dynamic spatial-embedding fusion network. *IEEE Trans. Multimed.*, 26:367–378, 2024. **1**
- [36] Jia-Yi Li, Xile Zhao, Jian-Li Wang, Chao Wang, and Min Wang. Superpixel-informed implicit neural representation for multi-dimensional data. In Ales Leonardis, Elisa Ricci, Stefan Roth, Olga Russakovsky, Torsten Sattler, and Gül Varol, editors, *Computer Vision - ECCV 2024 - 18th European Conference, Milan, Italy, September 29–October 4, 2024, Proceedings, Part II*, volume 15060 of *Lecture Notes in Computer Science*, pages 258–276. Springer, 2024. **3**
- [37] Xin Li, Shenqi Lai, and Xueming Qian. Dbcface: Towards pure convolutional neural network face detection. *IEEE Trans. Circuits Syst. Video Technol.(TCSVT)*, pages 1–1, 2021. **3**
- [38] Zhengqin Li and Jiansheng Chen. Superpixel segmentation using linear spectral clustering. In *IEEE Conference on Computer Vision and Pattern Recognition (CVPR)*, pages 1356–1363, 2015. **1, 2, 7**
- [39] Zhenguo Li, Xiao-Ming Wu, and Shih-Fu Chang. Segmentation using superpixels: A bipartite graph partitioning approach. In *IEEE Conference on Computer Vision and Pattern Recognition (CVPR)*, pages 789–796, June 2012. **3**
- [40] Chengxu Liu, Yuanzhi Liang, Yao Xue, Xueming Qian, and Jianlong Fu. Food and ingredient joint learning for fine-grained recognition. *IEEE Trans. Circuits Syst. Video Technol.(TCSVT)*, 31(6):2480–2493, 2021. **3**
- [41] Jiyuan Liu, Xinwang Liu, Siwei Wang, Sihang Zhou, and Yuexiang Yang. Hierarchical multiple kernel clustering. In *AAAI Conference on Artificial Intelligence (AAAI)*, pages 8671–8679, 2021. **5**
- [42] Ming-Yu Liu, Oncel Tuzel, Srikumar Ramalingam, and Rama Chellappa. Entropy rate superpixel segmentation. In *IEEE Conference on Computer Vision and Pattern Recognition, (CVPR)*, pages 2097–2104, 2011. **1, 2, 7**
- [43] Yun Liu, Peng-Tao Jiang, Vahan Petrosyan, Shi-Jie Li, Jiawang Bian, Le Zhang, and Ming-Ming Cheng. DEL: deep embedding learning for efficient image segmentation. In *International Joint Conference on Artificial Intelligence (IJCAI)*, pages 864–870, 2018. **3, 9, 10**
- [44] Yong-Jin Liu, Cheng-Chi Yu, Mingjing Yu, and Ying He. Manifold SLIC: A fast method to compute content-sensitive superpixels. In *IEEE Conference on Computer Vision and Pattern Recognition (CVPR)*, pages 651–659, 2016. **1, 2**
- [45] Jiangbo Lu, Hongsheng Yang, Dongbo Min, and Minh N. Do. Patch match filter: Efficient edge-aware filtering meets randomized search for fast correspondence field estimation. In *IEEE Conference on Computer Vision and Pattern Recognition (CVPR)*, pages 1854–1861, June 2013. **1**
- [46] Vaia Machairas, Matthieu Faessel, David Cárdenas-Peña, Théodore Chabardès, Thomas Walter, and Etienne Decencière. Waterpixels. *IEEE Trans. Image Processing (TIP)*, 24(11):3707–3716, 2015. **2**
- [47] Sree Ramya S. P. Malladi, Sundaresh Ram, and Jeffrey J. Rodriguez. Image denoising using superpixel-based PCA. *IEEE Trans. Multimed.*, 23:2297–2309, 2021. **1**
- [48] Nikolaus Mayer, Eddy Ilg, Philip Häusser, Philipp Fischer, Daniel Cremers, Alexey Dosovitskiy, and Thomas Brox. A large dataset to train convolutional networks for disparity, optical flow, and scene flow estimation. In *IEEE Conference on Computer Vision and Pattern Recognition (CVPR)*, pages 4040–4048, 2016. **2, 11**
- [49] Cheng Ouyang, Carlo Biffi, Chen Chen, Turkey Kart, Huaqi Qiu, and Daniel Rueckert. Self-supervision with superpixels: Training few-shot medical image segmentation without annotation. In *European Conference on Computer Vision (ECCV)*, pages 762–780, 2020. **3**
- [50] Rafael Martínez García Peña, Mansoor Ali Tevno, Gilberto Ochoa-Ruiz, and Sharib Ali. SUPRA: superpixel guided loss for improved multi-modal segmentation in endoscopy. In *IEEE/CVF Conference on Computer Vision and Pattern Recognition, CVPR 2023 - Workshops, Vancouver, BC, Canada, June 17–24, 2023*, pages 285–294. IEEE, 2023. **1**
- [51] Xiaofeng Ren and Jitendra Malik. Learning a classification model for segmentation. In *IEEE International Conference on Computer Vision (ICCV)*, pages 10–17, 2003. **1**
- [52] Olaf Ronneberger, Philipp Fischer, and Thomas Brox. U-net: Convolutional networks for biomedical image segmentation. In *Medical Image Computing and Computer-Assisted Intervention (MICCAI)*, volume 9351, pages 234–241, 2015. **1**
- [53] Abhishek Sharma, Oncel Tuzel, and Ming-Yu Liu. Recursive context propagation network for semantic scene labeling. In *Advances in Neural Information Processing Systems (NeurIPS)*, pages 2447–2455, 2014. **1**
- [54] Evan Shelhamer, Jonathan Long, and Trevor Darrell. Fully convolutional networks for semantic segmentation. *IEEE Trans. Pattern Anal. Mach. Intell. (TPAMI)*, 39(4):640–651, 2017. **1**
- [55] Nathan Silberman, Derek Hoiem, Pushmeet Kohli, and Rob Fergus. Indoor segmentation and support inference from RGBD images. In *European Conference on Computer Vision (ECCV)*, volume 7576, pages 746–760, 2012. **2, 5**
- [56] David Stutz, Alexander Hermans, and Bastian Leibe. Superpixels: An evaluation of the state-of-the-art. *Comput. Vis. Image Underst.*, 166:1–27, 2018. **2, 5**
- [57] Deqing Sun, Ce Liu, and Hanspeter Pfister. Local layering for joint motion estimation and occlusion detection. In *IEEE Conference on Computer Vision and Pattern Recognition (CVPR)*, pages 1098–1105, June 2014. **1**
- [58] Wen Sun, Qingmin Liao, Jing-Hao Xue, and Fei Zhou. SPSIM: A superpixel-based similarity index for full-reference image quality assessment. *IEEE Trans. Image Processing (TIP)*, 27(9):4232–4244, 2018. **3**
- [59] Teppei Suzuki, Shuichi Akizuki, Naoki Kato, and Yoshimitsu Aoki. Superpixel convolution for segmentation. In *International Conference on Image Processing (ICIP)*, pages 3249–3253, Oct 2018. **1**
- [60] Wei-Chih Tu, Ming-Yu Liu, Varun Jampani, Deqing Sun, Shao-Yi

- Chien, Ming-Hsuan Yang, and Jan Kautz. Learning superpixels with segmentation-aware affinity loss. In *IEEE Conference on Computer Vision and Pattern Recognition, (CVPR)*, pages 568–576, 2018. **3, 5, 7**
- [61] Olga Veksler, Yuri Boykov, and Paria Mehrani. Superpixels and super-voxels in an energy optimization framework. In *European Conference on Computer Vision (ECCV)*, pages 211–224, Sep. 2010. **2**
- [62] Hui Wang, Jianbing Shen, Junbo Yin, Xingping Dong, Hanqiu Sun, and Ling Shao. Adaptive nonlocal random walks for image superpixel segmentation. *IEEE Trans. Circuits Syst. Video Technol.(TCSVT)*, 30(3):822–834, 2020. **3**
- [63] Jingdong Wang, Ke Sun, Tianheng Cheng, Borui Jiang, Chaorui Deng, Yang Zhao, Dong Liu, Yadong Mu, Mingkui Tan, Xinggang Wang, Wenyu Liu, and Bin Xiao. Deep high-resolution representation learning for visual recognition. *IEEE Trans. Pattern Anal. Mach. Intell. (TPAMI)*, pages 1–1, 2020. **3**
- [64] Yaxiong Wang, Yunchao Wei, Xueming Qian, Li Zhu, and Yi Yang. Association implantation for superpixel segmentation. In *IEEE International Conference on Computer Vision (ICCV)*, Oct. 2021. **2, 7, 8**
- [65] Yunchao Wei, Xiaodan Liang, Yunpeng Chen, Xiaohui Shen, Ming-Ming Cheng, Jiashi Feng, Yao Zhao, and Shuicheng Yan. STC: A simple to complex framework for weakly-supervised semantic segmentation. *IEEE Trans. Pattern Anal. Mach. Intell. (TPAMI)*, 39(11):2314–2320. **3**
- [66] Koichiro Yamaguchi, David A. McAllester, and Raquel Urtasun. Robust monocular epipolar flow estimation. In *IEEE Conference on Computer Vision and Pattern Recognition (CVPR)*, pages 1862–1869, June 2013. **1**
- [67] Chuan Yang, Lihe Zhang, Huchuan Lu, Xiang Ruan, and Ming-Hsuan Yang. Saliency detection via graph-based manifold ranking. volume 22, pages 885–896, 2020. **1**
- [68] Fengting Yang, Qian Sun, Hailin Jin, and Zihan Zhou. Superpixel segmentation with fully convolutional networks. In *IEEE Conference on Computer Vision and Pattern Recognition, (CVPR)*, pages 13961–13970, 2020. **1, 3, 4, 5, 6, 7, 8, 9, 11**
- [69] Gengshan Yang, Joshua Manela, Michael Happold, and Deva Ramanan. Hierarchical deep stereo matching on high-resolution images. In *IEEE Conference on Computer Vision and Pattern Recognition (CVPR)*, pages 5515–5524, 2019. **2, 11**
- [70] Donghun Yeo, Jeany Son, Bohyung Han, and Joon Hee Han. Superpixel-based tracking-by-segmentation using markov chains. In *IEEE Conference on Computer Vision and Pattern Recognition (CVPR)*, pages 511–520, June 2017. **3**
- [71] Aiping Zhang, Wenqi Ren, Yi Liu, and Xiaochun Cao. Lightweight image super-resolution with superpixel token interaction. In *IEEE/CVF International Conference on Computer Vision, ICCV 2023, Paris, France, October 1-6, 2023*, pages 12682–12691. IEEE, 2023. **3**
- [72] Xiaolin Zhang, Yunchao Wei, Zhao Li, Chenggang Yan, and Yi Yang. Rich embedding features for one-shot semantic segmentation. *IEEE Trans. Neural Networks Learn.Syst. (TNNLS)*, pages 1–10, 2021. **3**
- [73] Chunhui Zhao, Boao Qin, Shou Feng, Wenxiang Zhu, Weiwei Sun, Wei Li, and Xiuping Jia. Hyperspectral image classification with multi-attention transformer and adaptive superpixel segmentation-based active learning. *IEEE Trans. Image Process.*, 32:3606–3621, 2023. **1**
- [74] Qiang Zhao, Feng Dai, Yike Ma, Liang Wan, Jiawan Zhang, and Yongdong Zhang. Spherical superpixel segmentation. *IEEE Trans. Multimed.*, 20(6):1406–1417, 2018. **1**
- [75] Zhedong Zheng and Yi Yang. Unsupervised scene adaptation with memory regularization in vivo. In *International Joint Conference on Artificial Intelligence (IJCAI)*, 2020. **1**
- [76] Zhedong Zheng and Yi Yang. Rectifying pseudo label learning via uncertainty estimation for domain adaptive semantic segmentation. *Int. J. Comput. Vis. (IJCV)*, 2021. **1**
- [77] Pei Zhou, Xuejing Kang, and Anlong Ming. Vine spread for superpixel segmentation. *IEEE Trans. Image Process.*, 32:878–891, 2023. **1**
- [78] Lei Zhu, Qi She, Bin Zhang, Yanye Lu, Zhilin Lu, Duo Li, and Jie Hu. Learning the superpixel in a non-iterative and lifelong manner. In *IEEE Conference on Computer Vision and Pattern Recognition (CVPR)*, pages 1225–1234, 2021. **3**
- [79] Wangjiang Zhu, Shuang Liang, Yichen Wei, and Jian Sun. Saliency optimization from robust background detection. In *IEEE Conference on Computer Vision and Pattern Recognition (CVPR)*, pages 2814–2821, 2014. **1**
- [80] Xizhou Zhu, Han Hu, Stephen Lin, and Jifeng Dai. Deformable convnets V2: more deformable, better results. In *IEEE Conference on Computer Vision and Pattern Recognition (CVPR)*, pages 9308–9316, 2019. **11**



Yaxiong Wang received the B.S. degree from Lanzhou University, Lanzhou, China, in 2015. He received his Ph.D degree at School of software Engineering, Xi'an Jiaotong University, Xi'an, China. He is now an assistant professor of Hefei University of Technology, Hefei, China. His current research interests include cross-modal retrieval, image generation, and AIGC detection.



Career Researcher Award Fellow from 2019 to 2021.

Yunchao Wei received the Ph.D. degree from Beijing Jiaotong University, Beijing, China, in 2016. He is currently an Professor with the Beijing Jiaotong University, Beijing, China. Before joining the Beijing Jiaotong University, he was a lecturer with University of Technology Sydney, Sydney, Australia. He was a Postdoctoral Researcher with the Beckman Institute, University of Illinois at Urbana-Champaign, Urbana, IL, USA, from 2017 to 2019. His current research interests include computer vision and machine learning. Dr. Wei is an ARC Discovery Early Career Researcher Award Fellow from 2019 to 2021.



Yujiao Wu received the Ph.D degree from University of Technology Sydney, Australia, in 2021. She is now a research scientist in CSIRO, Australia. Her current research interests include cross-modal retrieval, person retrieval, medical data analysis, and object detection.



Xueming Qian (M'10) received the B.S. and M.S. degrees from the Xi'an University of Technology, Xi'an, China, in 1999 and 2004, respectively, and the Ph.D. degree from the School of Electronics and Information Engineering, Xi'an Jiaotong University, in 2008. He was a Visiting Scholar with Microsoft Research Asia from 2010 to 2011. He was an Assistant Professor with Xi'an Jiaotong University, where he was an Associate Professor from 2011 to 2014, and is currently a Full Professor. He is also the Director of the Smiles Laboratory at Xi'an Jiaotong University. He received the Microsoft Fellowship in 2006. He received outstanding doctoral dissertations of Xi'an Jiaotong University and Shaanxi Province, in 2010 and 2011, respectively. His research interests include social media big data mining and search. His research is supported by the National Natural Science Foundation of China, Microsoft Research, and Ministry of Science and Technology.



Li Zhu is an associate professor in School of Software, Xi'an Jiao-tong University. He received his M.S. and Ph.D. degrees from Xi'an Jiaotong University in 1995 and 2000, respectively. He received his B.S. degree from Northwestern Polytechnical University in 1989. His main research interests include multimedia processing & communication, parallel computing and networking.



Yi Yang received the Ph.D. degree in computer science from Zhejiang University, Hangzhou, China, in 2010. He is currently a Professor with Zhejiang University, Hangzhou, China. Before joining the Zhejiang University, he served as a professor with the University of Technology Sydney, Sydney, NSW, Australia. He was a Postdoctoral Researcher with the School of Computer Science, Carnegie Mellon University, Pittsburgh, PA, USA. His current research interests include machine learning and its applications to multimedia content analysis and computer vision, such as multimedia indexing and retrieval, surveillance video analysis, and video semantics understanding.